# CALCULATION OF THE SECOND AER KINETIC BENCHMARK PROBLEM BY USING A NEW NODAL METHOD

**István Pataki, András Keresztúri**

Centre for Energy Research, Hungarian Academy of Sciences,
Reactor Analysis Department,
H-1525 Budapest 114, P.O. Box 49, Hungary
pataki@sunserv.kfki.hu

## ABSTRACT

A new, multigroup version of the KIKO3D code allowing arbitrary number of energy groups – called KIKO3DMG – was developed for calculation of the fast spectrum reactors. From among the advanced new features, the possibility of using triangular geometry and the automated cutting the triangles into further ones at many levels was utilized for an attempt to reach a converged solution of the Second AER Kinetic Benchmark Problem.

## 1. INTRODUCTION

From the 1990's, several kinetic and dynamic benchmark problems have been defined in the frame of the AER (Atomic Energy Research) cooperation. Most of them can be classified into the group of the "numerical exercise benchmarks" as far as measurements are not supporting them and - at the same time - some modeling details are entrusted to the participants. Although the most important "integral" modeling features are "normalized" in the definitions (shut down margin, recriticality temperature, advised thermal hydraulic correlations, etc.), in the strict sense the abovementioned feature prevails starting from the third AER kinetic benchamark concerning the not fully exact prescription of the cross sections or all the details of the thermal hydraulic modeling. (An advantage of these characteristics must also mentioned, namely this approach is representing the real situation concerning the modeling uncertainties as far as the variance of the different solutions is regarded.) The first and second kinetic benchmarks [1] are exceptions from this point of view because their definition makes it theoretically possible to have the converged reference solution. In this sense, the two latter mentioned benchmarks can be regarded as "mathematical benchmarks" in close relation with their relative simplicity. Nevertheless, the efforts for determining their converged reference solutions seem not fully satisfactory, especially regarding the AER Benchmark Book („http://aerbench.kfki.hu/aerbench/ "). A very important, large step in this direction was made by N. Kolev, R. Lenain, and C. Magnaud calculating the second kinetic benchmark by using the CRONOS fine-mesh method [2]. An extrapolated to zero mesh size reference solution was recommended for the steady states and it revealed significant deviations from the solutions obtained from the nodal codes. The significant deviation raised certain doubts in some participants concerning the advised reference solution. The goal of the present work is to contribute to the existence of the reference solution of the second kinetic rod ejection benchmark in the AER Benchmark Book.

Another motivation of the present work is that a new version of the KIKO3D code – called KIKO3DMG – has been developed which is applicable also for triangular geometry and the automated cutting the triangles into further ones at many levels (see Fig. 1) is also supported. This new feature could be utilized for an attempt to reach a converged solution of the Second AER Kinetic Benchmark Problem.



| 6 triangles | 24 triangles | 96 triangles | 384 triangles | 1536 triangles |
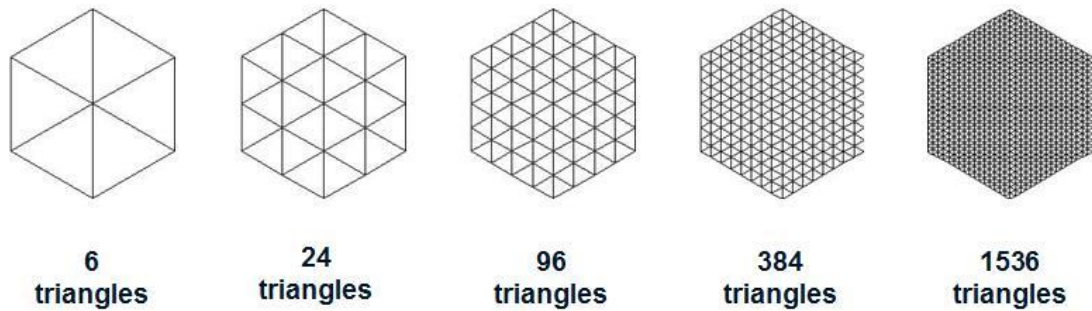
**Figure 1** Subdivision of the hexagons into triangles

## 2. THE TRIANGULAR GEOMETRY NODAL METHOD OF KIKO3DMG CODE

The basic theoretical assumptions of the old KIKO3D are as follows [3]:
- Two energy groups, homogenized assemblies, hexagonal and square geometry
- Nodal method: the nodes are the fuel assemblies subdivided by axial layers-
- **The unknowns are the scalar flux integrals on the node interfaces.**
- Linear anisotropy of the angle dependent flux on the node boundaries assumed
- Nodal equations obtained from the condition that the scalar flux and net current integrals are continuous on the node interfaces
- **Analytical solutions of the diffusion equation inside the nodes: exponential or/and trigonometric "wave functions" perpendicular to the node interfaces**
- Generalized response matrices of the time dependent problem and time dependent nodal equations
- IQS (Improved Quasi Static) factorization; shape function equations and point kinetic equations
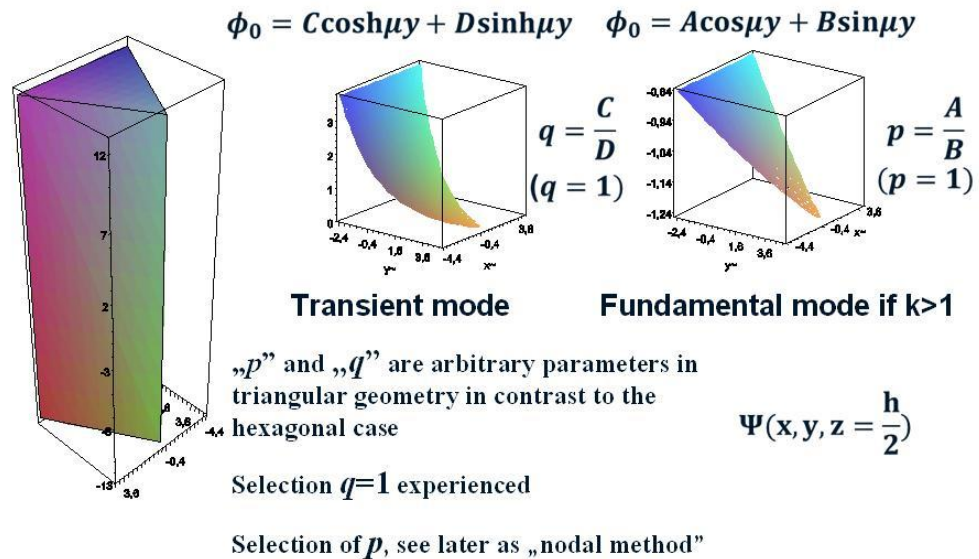- The absorbers and the reflector represented by pre-calculated albedo matrices.

In the advanced version – KIKO3DMG - the basic theoretical assumptions of the older version were kept, but the following developments have been elaborated:
- Arbitrary number of energy groups → fast spectrum reactor applications
- Possibility of the up-scattering → more than one thermal group, more accurate calculations of the thermal reactors in the vicinity of the reflector
- Supported geometries: hexagonal, square, **triangular**, slab
- **Optimized iterations for multi-thread processing**
- Graphical output for radial distributions (flux, power, temp., kq, etc.),

- **Hexagonal geometry input can be cut into triangular pieces in an automated way.**
- **The hexagonal output can be synthesized from the triangular results.**

The new advanced features highlighted above made the convergence investigations possible by applying a step by step nodalization refinement.

# Flux distributions inside the nodes



$$\phi_0 = C\cosh\mu y + D\sinh\mu y \qquad \phi_0 = A\cos\mu y + B\sin\mu y$$

$$q = \frac{C}{D}$$
$$(q = 1)$$

$$p = \frac{A}{B}$$
$$(p = 1)$$

**Transient mode**     **Fundamental mode if k>1**

„*p*" and „*q*" are arbitrary parameters in triangular geometry in contrast to the hexagonal case

$$\Psi(x, y, z = \frac{h}{2})$$

Selection *q*=1 experienced

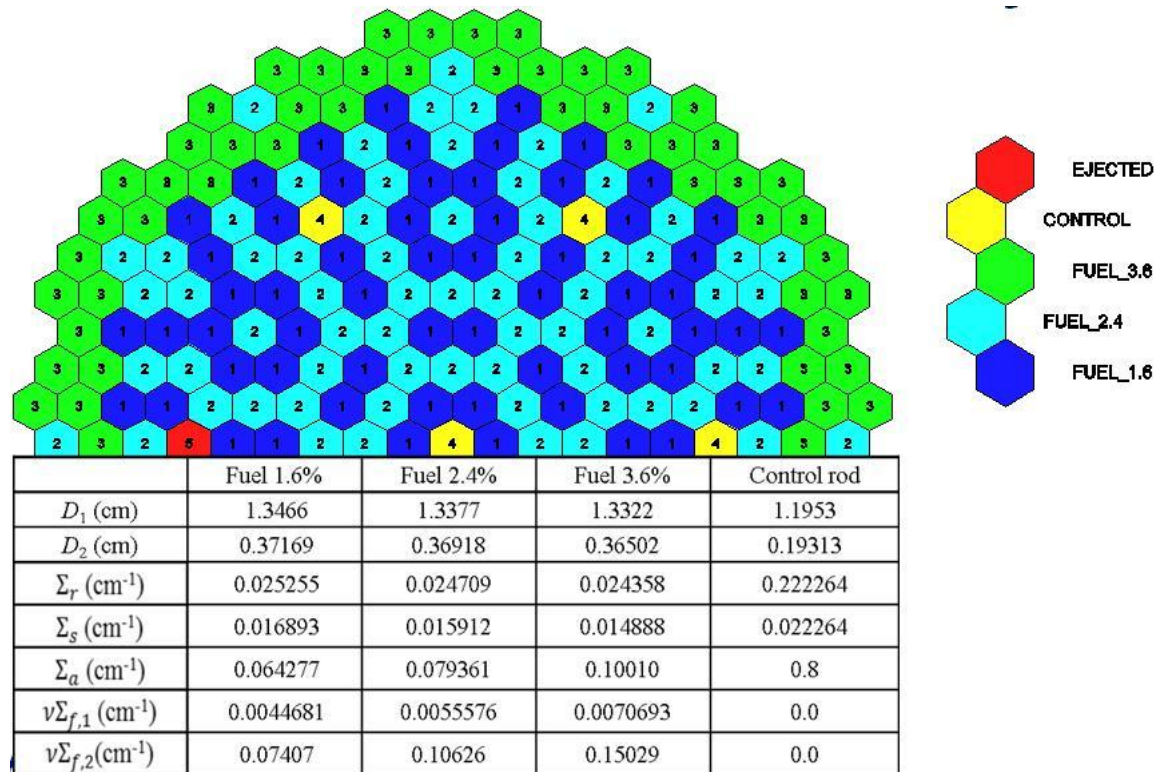Selection of *p*, see later as „nodal method"

**Figure 2** Flux distributions in the triangle nodes

The solutions of the diffusion equation inside a node in case of the triangular geometry are illustrated in Fig. 2. According to the assumptions highlighted in connection with the older version and kept also in case of the new one, the number of freedom of the different solutions is equal to four times the different directions perpendicular to the node boundaries. It is 4*3=12 - in 2D geometry - in case in of the hexagonal geometry and - originally - the same (!) for the triangular geometry. (The 2D geometry is used here only for the simplification of the explanation.) On the other hand, the number of unknowns – the scalar flux integrals at the node boundaries - is twice the node boundaries for both cases, which is 12 for the hexagonal and 6 for the triangular geometry. This way, the number of the unknowns and the number of the freedom of the solutions are the same for the original hexagonal geometry, while in case of the triangular geometry - originally - there are twice as many different modes than the number of unknowns (the latter one determined from the equality of the partial currents). This is the reason why the quantities "*q*" and "*p*" on Fig. 2 are theoretically arbitrary, and their predetermined all combinations are representing different nodal methods. Our preliminary trials proved that for the transient modes the *q*=1 is an appropriate selection while the appropriate value "*p*" was a subject of the investigations discussed in the next sections.

# 3. THE AER-2 DYNAMIC BENCHMARK PROBLEM

The second kinetic benchmark [1] aims at the validation of 3D neutron kinetics calculations for VVER-440 with a simplified, "adiabatic" fuel temperature feedback. The transient is an asymmetric control rod ejection. The benchmark has two variants for handling the control assemblies (according to the different abilities of the participating codes): (A) by two-group constants or (B) by albedo matrices. The worth of the ejected rod is 2$. The initial power is close to zero. The rod is ejected during the first 0.16 s, and the transient is followed until 2 s without scram. The horizontal and vertical geometry are shown in Figs. 1 and 2 and further data of the benchmark are presented in Table 1.



|  | Fuel 1.6% | Fuel 2.4% | Fuel 3.6% | Control rod |
|---|---|---|---|---|
| $D_1$ (cm) | 1.3466 | 1.3377 | 1.3322 | 1.1953 |
| $D_2$ (cm) | 0.37169 | 0.36918 | 0.36502 | 0.19313 |
| $\Sigma_r$ (cm$^{-1}$) | 0.025255 | 0.024709 | 0.024358 | 0.222264 |
| $\Sigma_s$ (cm$^{-1}$) | 0.016893 | 0.015912 | 0.014888 | 0.022264 |
| $\Sigma_a$ (cm$^{-1}$) | 0.064277 | 0.079361 | 0.10010 | 0.8 |
| $\nu\Sigma_{f,1}$ (cm$^{-1}$) | 0.0044681 | 0.0055576 | 0.0070693 | 0.0 |
| $\nu\Sigma_{f,2}$ (cm$^{-1}$) | 0.07407 | 0.10626 | 0.15029 | 0.0 |

**Figure 3** Horizontal layout of the half core of the AER-2 dynamic benchmark

**Table 1** Main characteristics of the AER-2 dynamic benchmark

| Parameter | Value |
|---|---|
| Ejection time of absorber | 0.16 s |
| Subassembly pitch | 14.7 cm |
| Height of core | 250 cm |
| Number of pins per fuel assembly | 126 |
| Outer diameter of fuel pellet | 0.76 cm |

| | |
|---|---|
| Inner diameter of fuel pellet | 0.14 cm |
| Density of fuel | 10.4 g/cm3 |
| Heat capacity of fuel | 0.3 J/(g oC) |
| Beff | 0.005 |
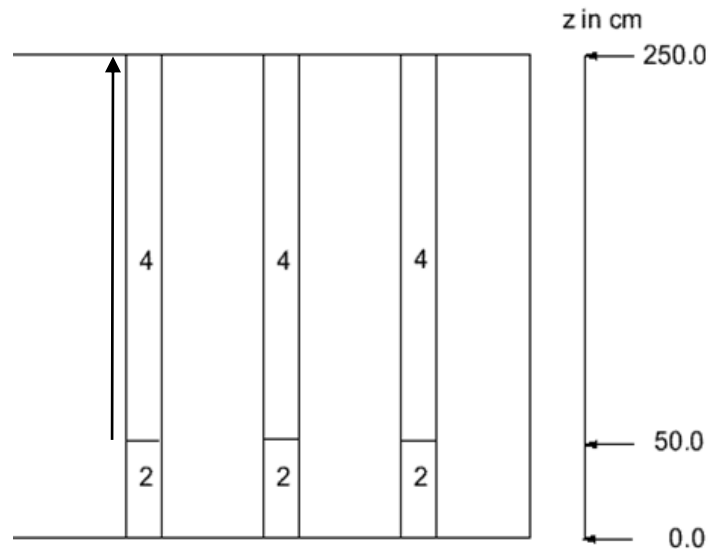
**Figure 4** Vertical layout of the half core of the AER-2 dynamic benchmark

It was found that the power peak caused by the rod ejection is in close relation with the static worth of the ejected rod. Therefore, first the different solutions were compared on this level. The various static nodal solutions were summarized in the paper [2] according to Table 2, where additionally an extrapolated to zero mesh size reference solution was recommended for the steady states and it revealed significant deviations from the solutions obtained from the nodal codes. Although some dynamical solutions obtained from KIKO3DMG are presented in the further parts of the paper, it focuses also on the static reactivity values.

**Table 2** Main characteristics of the AER-2 dynamic benchmark

| CODE | keff,0 | keff,1 | Δρ (%) | Δρ/Δρref - 1(%) |
|---|---|---|---|---|
| BIPR8 | 0.998442 | 1.008673 | 1.01589% | -3.74% |
| DYN3D | 0.999941 | 1.009792 | 0.97561% | -7.56% |
| HEXNEM2 | 0.999112 | 1.009417 | 1.02179% | -3.18% |
| HEXTRAN | 0.99902 | 1.009181 | 1.00784% | -4.50% |
| KIKO3D | 0.999994 | 1.009926 | 0.98344% | -6.82% |
| SKETCH | 0.99841 | 1.00872 | 1.02372% | -3.00% |
| CRONOS | 0.99784 | 1.00846 | 1.05537 % | 0.00% |

## 4. THE SOLUTIONS OBTAINED FROM KIKO3DMG

The influence of the mesh refinement was investigated in two steps. It was found that the multiplication factors (and the distributions, too) are more sensitive to the radial mesh refinement than the axial nodalization. Therefore, first, the appropriate mesh (number of triangles) and nodal method ("*p*" parameter) were determined and the influence of the axial mesh refinement was investigated only in the second phase.

## 4.1 Radial mesh refinement results

In the investigations of point 4.1, the assemblies were subdivided into 10 axial nodes.

In Fig. 5, the effective multiplication factors for the symmetric steady state (before the transient) are shown for the different nodal methods – represented by the different "$p$" values – and for the different radial nodalizations. According to the figure, the convergence of each nodal method is observed when the nodalization was refined systematically. Nevertheless, taking into account the sensitivity of the power peak maximum on the multiplication factors, the differences seem not negligible, therefore, in order to find the converged solution in an acceptable computer time, it was important to find an appropriate "$p$" value. Fig. 6 shows the maximum differences of the normalized power distributions from reference of the 1536 triangle calculation in the percent of the maximum local power. Although for the less detailed nodalization a small negative value of $p$ seems optimal, the figure shows that the optimum values of $p$ is shifted into the positive region when the number of triangles is increased and for the most detailed nodalization of Fig. 6 is close to 1.0. Mostly this value was used in the further investigations of the paper.
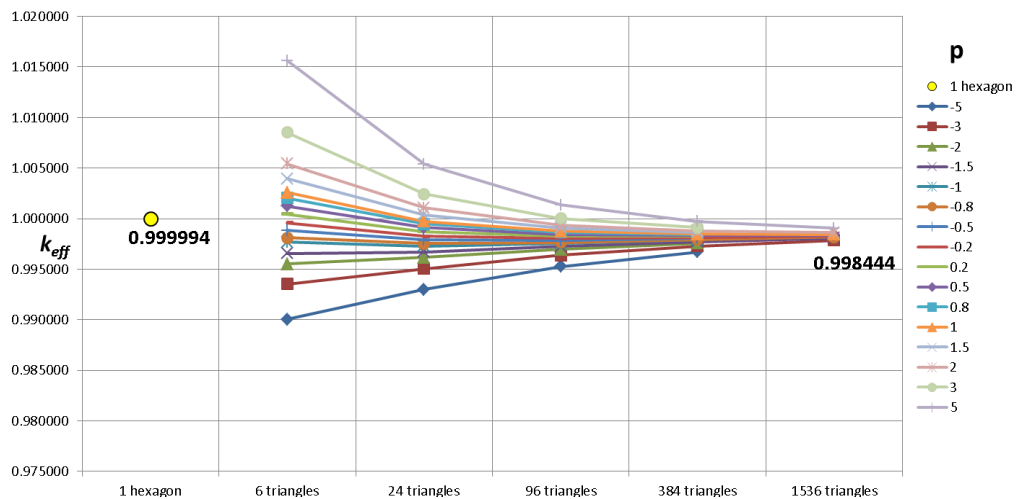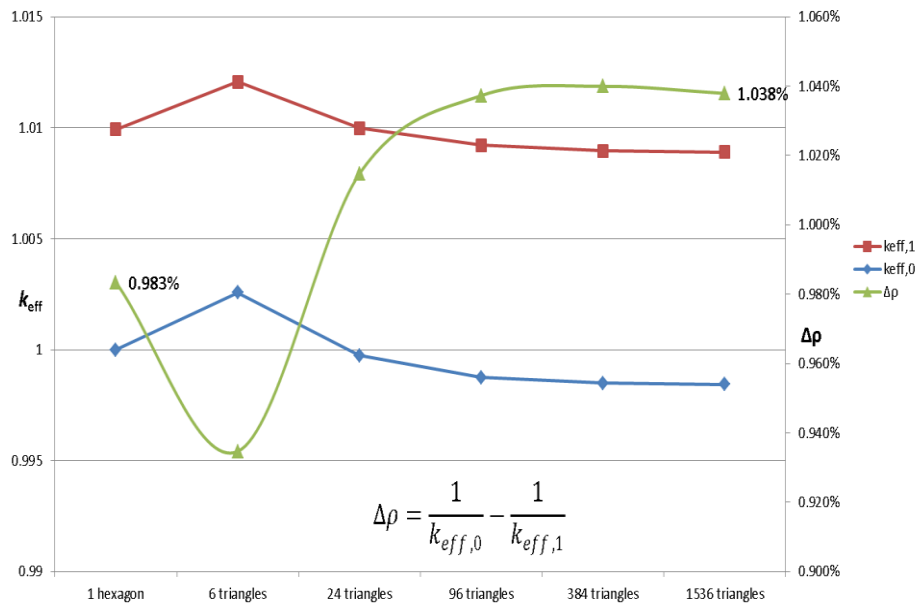


**Figure 5** Effective multiplication factors for the symmetric steady state (before the transient) by using different nodal methods – represented by the different "$p$" values – and with different radial nodalizations, the latter one characterized by the number of triangles in the hexagonal nodes
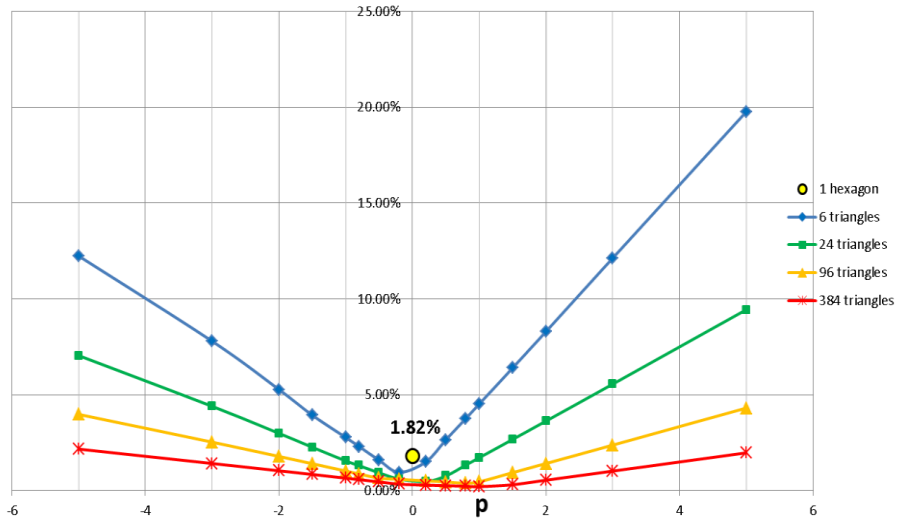
**Figure 6** Maximum differences of the normalized power distributions from the reference of the 1536 triangle calculation in the percent of the maximum local power



**Figure 7** Effective multiplication factors for the initial state and for the state when the control rod was ejected (left axis); the difference, namely the ejected rod worth („Δρ",
right axis) depending on the subdivision for $p = 1$ and $q = 1$
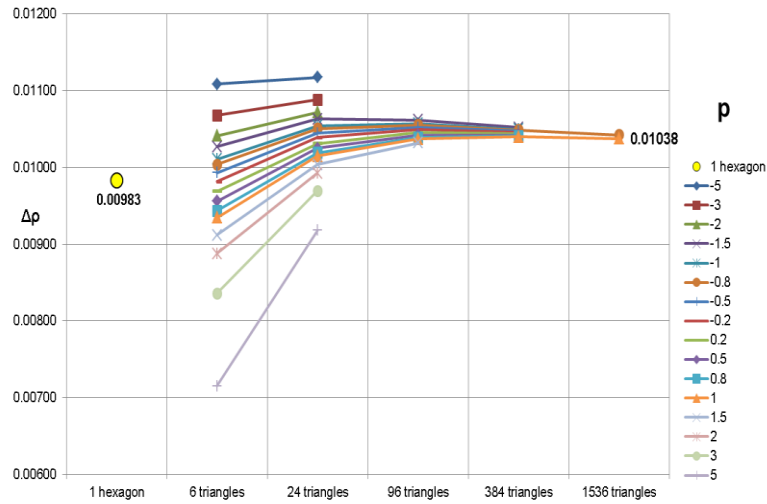
**Figure 8** Control rod worth depending on the subdivision and the nodal method, the latter one characterized by the p variable (q=1, number of axial layers = 10)

Figs 7 and 8 show the static reactivity worth of the ejected rod depending on the number of triangles in a hexagonal node at various values of "*p*". A convergence is observed, namely the reactivity is 1.038 % if the number of the triangles is 1536 and *p* = 1. The figures show also that practically the same value is obtained when *p* = -0.8 or the number of triangles is less, namely 384. Figure 9 shows the time dependent integral power at various number of triangles and values of *p*, and it manifests that the power peak is converged already when even less, namely 96 triangles are applied if *p* is in the range of 0.5 and 1.0. According to Fig. 10, the same conclusion can be drawn if the power peak obtained from the dynamic calculation is plotted as the function of the static worth of the ejected rod.
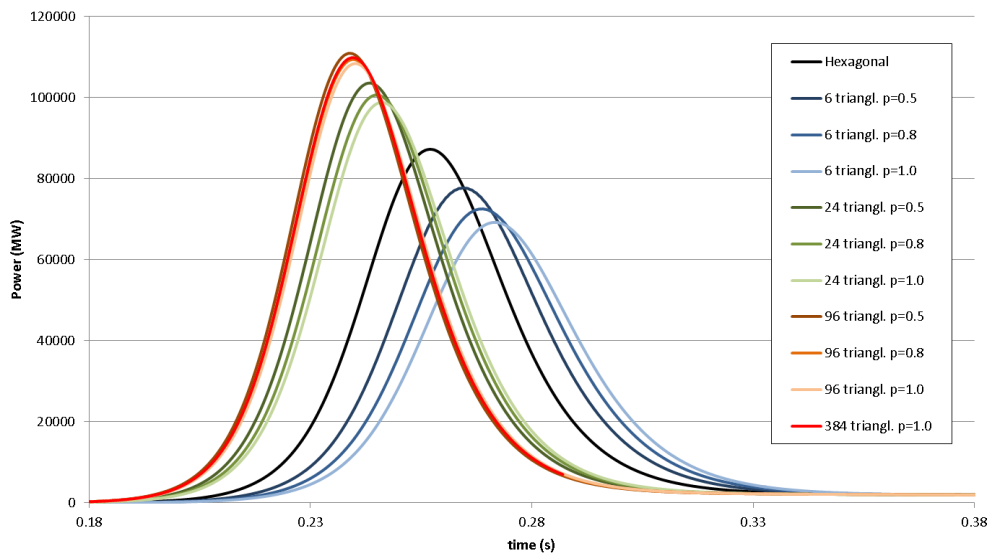


**Figure 9** The time dependent integral power at various number of triangles and values of *p*
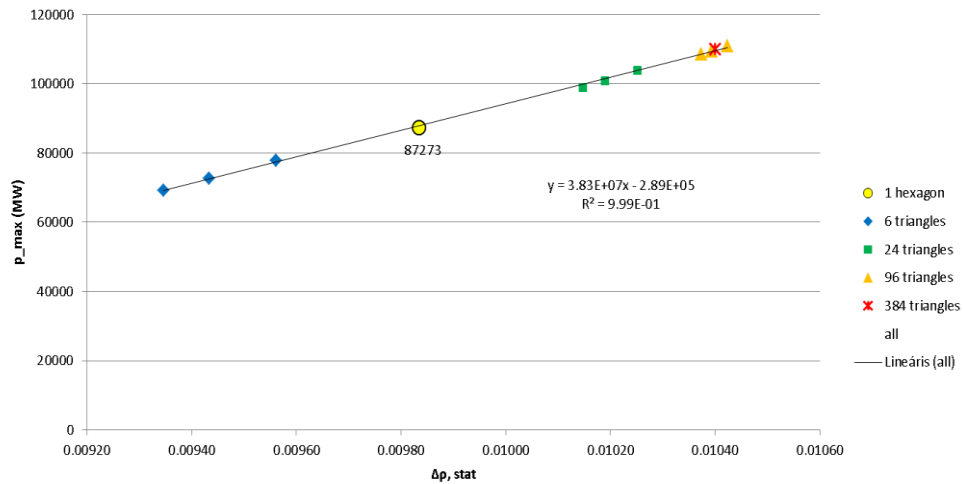
**Figure 10** Dependence of the power peak obtained from the dynamic calculation on the static worth of the ejected rod

## 4.2 Axial mesh refinement results

The calculations shown in Fig. 7 for 10 axial layers were repeated with increased axial subdivision and presented – together with the original curves – in Fig. 10. The static control rod worth was increased significantly – from 1.038 % to 1.0541 % - when the number of the axial nodes is increased from 10 to 25. No further improvement could be achieved in case of further axial mesh refinement from 25 to 50.
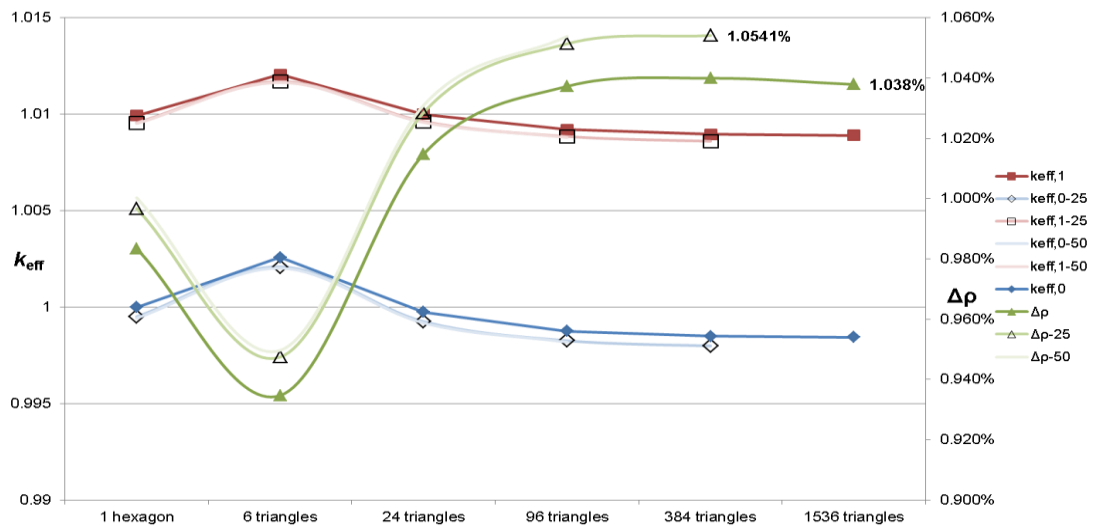


**Figure 11** Effective multiplication factors for the initial state and for the state when the control rod was ejected (left axis) for different axial nodalizations; the difference, namely the ejected rod worth („Δρ", right axis) depending on the subdivision for $p = 1$ and $q = 1$

# 5. SUMMARY AND CONCLUSIONS

The possibility in the KIKO3DMG code for using triangular geometry and the automated cutting the triangles into further ones at many levels was utilized to reach a converged solution of the Second AER Kinetic Benchmark Problem. It was found that both the static worth of the ejected rod and the maximum of the reactivity power are increasing continuously if the mesh is being refined systematically, nevertheless a convergence could be reached. The most important results are summarized in Table 3 and show that the converged solution is very close to that obtained in [2].

**Table 3** Summary of the KIKO3DMG results

| Method** | $k_{eff,0}$ | $K_{eff,1}$ | $\Delta\rho$ (%) | $\Delta\rho/\Delta\rho_{ref}$ - 1 (%) | pmax (MW) | pmax/pmax,ref -1 (%) |
|---|---|---|---|---|---|---|
| Hex. geom. | 0.999994 | 1.009926 | 0.98344 | 6.71% | 87273 | -24.00% |
| 24.10 | 0.999746 | 1.009992365 | 1.01476 | 3.74% | 98815 | -13.95% |
| 96.10 | 0.998757 | 1.009212061 | 1.03728 | 1.60% | 108410 | -5.59% |
| 384.10 | 0.998486 | 1.008962938 | 1.03996 | 1.35% | 109900 | -4.29% |
| 1536.10 | 0.998444 | 1.008899219 | 1.03791 | 1.54% | 108611* | -5.41% |
| 96.25 | 0.998261 | 1.00884992 | 1.05140 | 0.26% | 113777* | -0.92% |
| 96.50 | 0.998188 | 1.00879976 | 1.05387 | 0.03% | 114724* | -0.09% |
| 384.25*** | 0.99799 | 1.00860062 | 1.05415 | 0.00% | 114828* | 0.00% |

\* Extrapolated from the $\Delta\rho/\Delta\rho_{ref}$ values by using the curve of Fig. 1
\*\* XX.YY, where XX is the number of the triangles/node, YY is number of the axial subdivision
\*\*\* Regarded as converged solution

## REFERENCES

[1] U. Grundman and U. Rohde, Definition of the second hexagonal kinetic benchmark of AER, Proceedings of the 3rd Symposium of AER, 1993, pp. 325/332, KFKI Atomenergia Press, Budapest, 1993.

[2] N.P. Kolev R. Lenain, C.Fedon-Magnaud , Finite element solutions of the AER-2 rod ejection benchmark by CRONOS , Proceedings of the 11th Symposium of AER, 2001, pp. 395/411, KFKI Atomenergia Press, Budapest, 2001.

[3] A. Keresztúri, Gy. Hegyi, Cs. Maráczy, I. Panka, M.Telbisz, I. Trosztel and Cs. Hegedűs: Development and validation of the three-dimensional dynamic code - KIKO3D Annals of Nuclear Energy 30 (2003) pp. 93-120.